

UDC 547.314.2:546.62-311

<https://doi.org/10.15407/kataliz2025.36.057>

Catalytic properties of reduced graphene oxide deposited on aluminum and magnesium oxides in acetylene hydrogenation

Viktoriia V. Nosach^{1,2}, Igor B. Bychko¹, Peter Ye. Strizhak¹

¹ L.V. Pisarzhevskii Institute of Physical Chemistry of National Academy of Sciences of Ukraine
31 Nauky Avenue, Kyiv, 03028, Ukraine

² National University of "Kyiv-Mohyla Academy"

2 Hryhoriya Skovorody Str., Kyiv, 04655 Ukraine, e-mail: victorynosach@gmail.com

The catalytic properties of reduced graphene oxide (rGO) deposited on aluminum and magnesium oxides were investigated in acetylene hydrogenation. Catalysts with different rGO loadings were prepared by impregnating γ -Al₂O₃ and MgO with aqueous graphene oxide suspensions, followed by reduction in hydrogen at 400 °C. The materials were characterized by FTIR, Raman spectroscopy, and SEM. FTIR spectra confirmed the successful deposition of rGO on both supports, and for MgO-based samples, FTIR also revealed partial hydration of surface Mg–O groups, forming Mg(OH)₂ and a hydroxide–graphene interfacial layer that improves anchoring and stabilizes the structure. Raman spectroscopy verified the formation of a graphene-based phase on both oxides and showed that the defect level of the deposited graphene remains constant with varying rGO loading. SEM analysis indicated that on MgO, rGO forms thin film-like structures and irregular folds that create partially covered regions, while on γ -Al₂O₃ it forms continuous films in some areas and isolated folds in others. Modification of γ -Al₂O₃ and MgO with rGO enhanced catalytic activity in acetylene hydrogenation, with the highest rates observed for samples with low rGO content. Both rGO/Al₂O₃ and rGO/MgO exhibited full (100 %) selectivity to ethylene in the 250–400 °C range. The improved performance is attributed to rGO-derived surface structures that ensure effective contact between carbon and oxide phases and facilitate activation of acetylene and hydrogen. Overall, the catalytic behavior of rGO-modified oxides is governed by the acid–base properties of the support and the structural features of the deposited graphene layer, which determine the activation temperature and thermal stability of the system.

Keywords: reduced graphene oxide, aluminum oxide, magnesium oxide, acetylene hydrogenation, carbocatalysis

Introduction

Catalytic hydrogenation of acetylene is an important reaction in both fine organic synthesis and industrial chemistry, particularly in the production of high-purity ethylene [1, 2]. Achieving high selectivity and activity in this reaction typically relies on oxide-supported catalysts such as γ -Al₂O₃, SiO₂, MgO, and TiO₂. In recent years, increasing attention has been devoted to catalytic systems modified with carbon nanostructures, which can improve the adsorption capacity and stability of active centers [3, 4].

Among carbon-based materials, reduced graphene oxide (rGO) has attracted considerable interest due to its high surface area, chemical stability, and ability to form hybrid interfaces with oxide supports [5, 6]. The deposition of rGO layers on oxide surfaces promotes the formation of heterogeneous interfaces that affect adsorption properties and surface reactivity [7]. Depending on the properties of rGO, the catalytic properties of such hybrid systems may vary substantially.

Although most studies have focused on metal-loaded rGO catalysts, several works have demonstrated that rGO itself can exhibit intrinsic catalytic activity in hydrogenation reactions without metallic components [8, 9]. Metal-free reduced graphene oxide has been shown to catalyze the hydrogenation of acetylene to ethylene and phenylacetylene to styrene. In addition, defect-rich or N-doped rGO materials have demonstrated activity in the hydrogenation of styrene and terminal alkynes

under mild conditions, highlighting the intrinsic catalytic potential of graphene-based systems [10]. These findings indicate that rGO can act not only as a conductive support but also as an active component in hydrogenation processes.

The aim of this work is to reveal the effect of reduced graphene oxide deposited on γ -Al₂O₃ and MgO on the catalytic properties of the resulting materials in the process of acetylene hydrogenation. Structural and morphological characterization of the samples was performed using FTIR, Raman spectroscopies, SEM analyses, and the temperature dependence of acetylene conversion was studied. The obtained results provide a comparative analysis of γ -Al₂O₃- and MgO-supported systems, highlighting the effect of the support on catalytic efficiency in acetylene hydrogenation.

Experiment

Catalyst samples with reduced graphene oxide were prepared by applying an aqueous suspension of graphene oxide (GO) with different concentrations onto MgO (Novohim, 98.5 %) and Al₂O₃ (Yug Sintez, 99.0 %). The GO suspension was obtained by of graphite oxide (GrO), which had been synthesized using a modified Hummers' method followed by ultrasonic treatment [11]. Powders of aluminum oxide and magnesium oxide with a particle size fraction of 0.25-0.5 mm were impregnated with the suspension at a ratio of 1 mL per 1 g of support. After impregnation, the samples were kept at 60 °C for 3 h and then reduced in a hydrogen flow at 400 °C for 2 h. A series of samples containing GO at 0.025 mg/g, 0.1 mg/g, and 1 mg/g were prepared. Each sample in the series was labeled according to the type of support, the type of graphene material, and its concentration in wt. %, for example: rGO(0.0025)/MgO, rGO(0.01)/Al₂O₃, etc.

The physicochemical properties of the obtained samples were investigated using Raman spectroscopy, Fourier transform infrared spectroscopy (FTIR), scanning electron microscopy (SEM), and low-temperature nitrogen adsorption-desorption analysis. The morphology and spatial distribution of elements in the samples containing reduced graphene oxide were examined by SEM using a MIRA3 Tescan microscope. FTIR spectra were recorded with a Perkin Elmer "Spectrum One" spectrometer in the range of 400-4000 cm⁻¹. Raman spectra were obtained at room temperature using a HORIBA Jobin-Yvon T64000 confocal dispersive spectrometer equipped with an Ar-Kr laser (excitation wavelength 488 nm, laser power 125 mW).

The catalytic activity of the samples in the acetylene hydrogenation reaction was studied under flow conditions using chromatographic control of the composition of the reaction mixture and the conversion products. The analysis was performed using a self-made assembly gas chromatograph equipped with a thermal conductivity detector and a PoraPak S chromatographic column. The catalyst was placed in a fixed-bed flow reactor between two layers of purified quartz. The acetylene hydrogenation reaction was carried out in the temperature range of 50-400 °C using a gas mixture containing 10 % C₂H₂ and 90 % H₂ at a total flow rate of 50 mL min⁻¹. Catalyst samples weighing 0.1-0.25 g were used in the experiments.

The rate of hydrogenation product formation was calculated according to equations (1) and (2)

$$r_c = \frac{n_a \cdot V_n}{22400 \cdot 60 \cdot m_c} \quad 1) \qquad r_g = \frac{n_a \cdot V_n}{22400 \cdot 60 \cdot m_g} \quad 2)$$

where, n_a - the molar fraction of the hydrogenation product in the gas mixture after passing through the reactor; V_n - the flow rate of the acetylene-hydrogen gas mixture, ml/min, m_c - the mass of the catalyst sample, g; m_g - is the mass of reduced graphene oxide (rGO) in the catalyst sample, g.

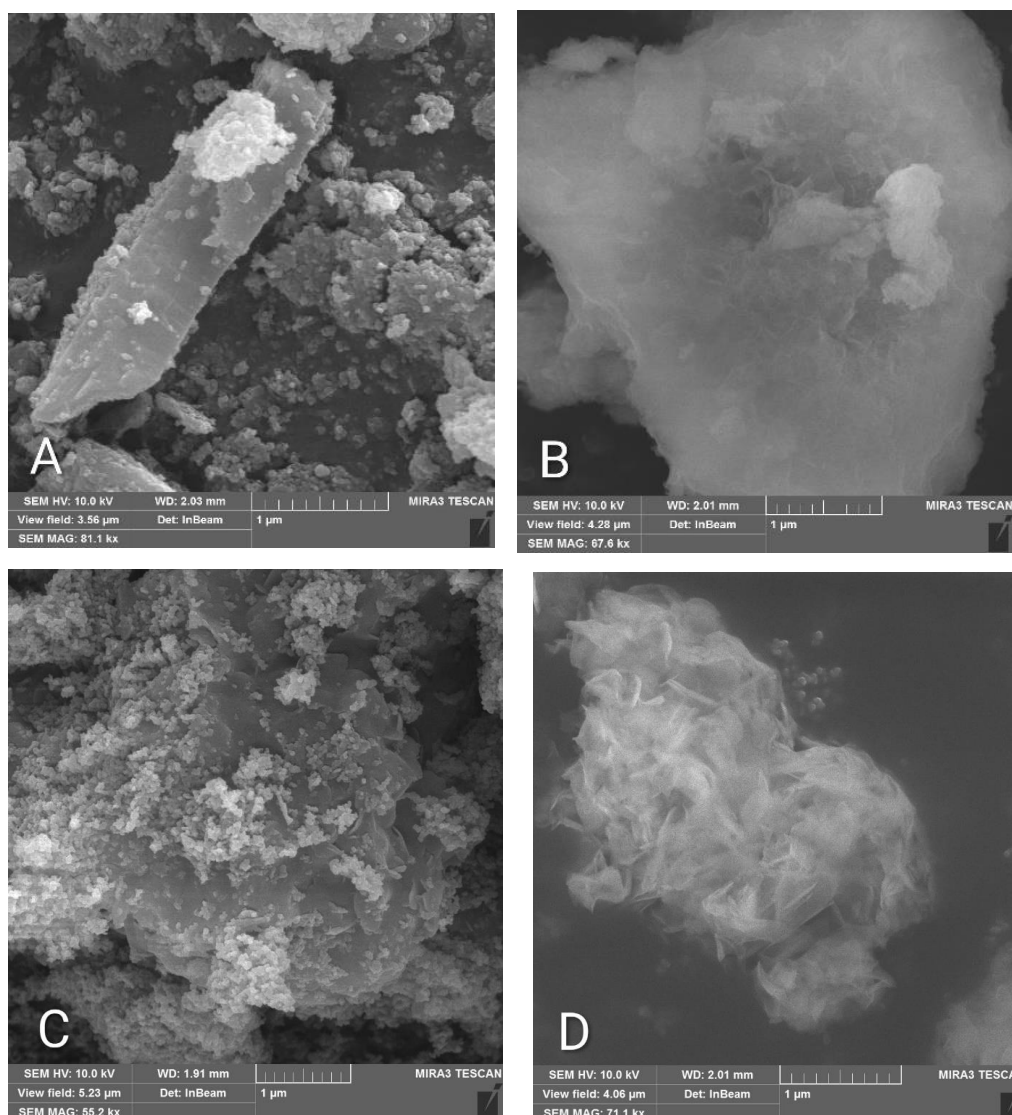


Fig. 1. SEM images of the samples: (a) Al_2O_3 ; (b) $\text{rGO}(0.1)/\text{Al}_2\text{O}_3$; (c) MgO ; (d) $\text{rGO}(0.1)/\text{MgO}$

Results and Discussion

Fig. 1 a, b shows the SEM images of pristine $\gamma\text{-Al}_2\text{O}_3$ and the $\gamma\text{-Al}_2\text{O}_3$ sample modified with rGO. The surface of the initial $\gamma\text{-Al}_2\text{O}_3$ is characterized by a porous structure formed by agglomerates of irregularly shaped nanoparticles [12]. After modification with rGO, film-like formations with a wrinkled texture, characteristic of graphene layers, appear on the oxide surface [13]. An uneven distribution of the rGO coating is observed: in some regions, rGO forms continuous films, whereas in others, isolated graphene folds and exposed areas of the alumina surface remain visible. Such morphology indicates a non-uniform deposition of rGO and partial coverage of the porous $\gamma\text{-Al}_2\text{O}_3$ surface.

Fig. 1 c, d presents the SEM images of pristine MgO and the MgO sample modified with reduced graphene oxide (rGO). The surface of the initial MgO consists of agglomerates of particles with well-defined cubic facets, typical of this oxide system [14]. After rGO deposition, noticeable changes occur in the surface morphology: thin film-like structures and folds corresponding to graphene layers appear on the granular MgO matrix. The rGO is distributed unevenly, forming localized regions with partial coverage of MgO grains, while some areas remain exposed. The formation of such hybrid regions

indicates weak interaction between the graphene layers and the MgO surface, which may result in differences in dispersion and interfacial contact compared to the Al₂O₃-rGO system.

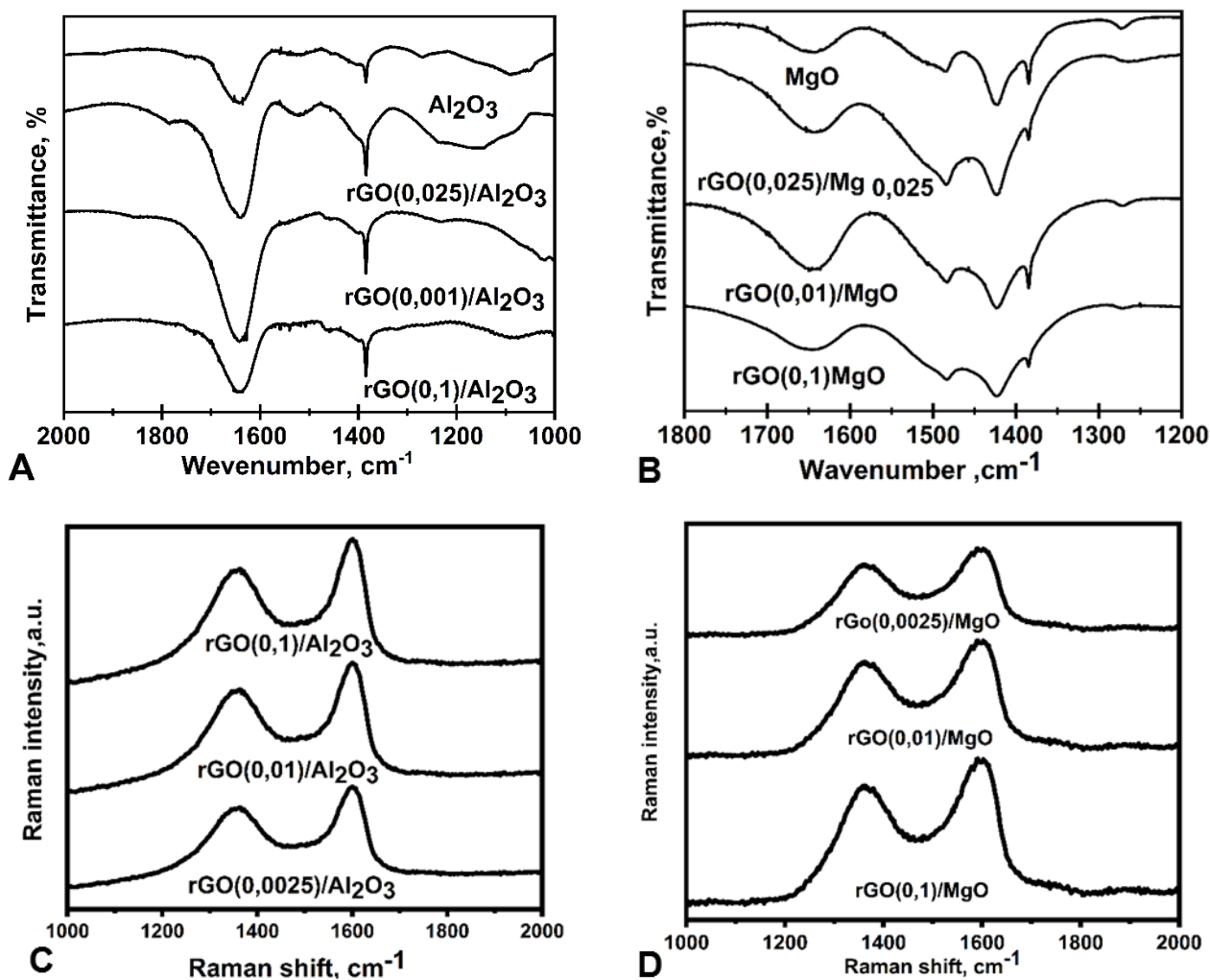


Fig. 2. FTIR (a) and Raman (b) spectra of rGO (0.0025)/Al₂O₃, rGO (0.01)/Al₂O₃, rGO (0.1)/Al₂O₃; FTIR (c) and Raman (d) spectra of (0.0025)/MgO, rGO (0.01)/MgO, rGO (0.1)/MgO

Fig. 2 a shows the FTIR spectra of pure γ -Al₂O₃ and the samples modified with different amounts of reduced graphene oxide. The spectrum of γ -Al₂O₃ reveals characteristic absorption bands in the region of 800-500 cm⁻¹, corresponding to the stretching and bending vibrations of Al-O and Al-O-Al bonds [15]. In the high-frequency region 3770-3700 cm⁻¹, sharp bands of isolated Al-OH groups are detected, while a broader feature near 3400 cm⁻¹ is attributed to hydrogen-bonded O-H groups and adsorbed water molecules. After the deposition of reduced graphene oxide, new absorption bands appear in the spectra. A weak band in the 1730-1710 cm⁻¹ region corresponds to the C=O stretching vibrations of carboxyl groups originating from residual oxygen-containing fragments of graphene oxide [16]. A distinct band at 1605-1585 cm⁻¹ is associated with C=C vibrations of the aromatic structure of graphene layers. In the region of 1260-1050 cm⁻¹, additional bands assigned to C-O-C vibrations of epoxy and ether groups, as well as C-O vibrations of phenolic groups, are observed. The O-H band in the high-frequency region becomes broader, suggesting the formation of hydrogen-bonded structures between the hydroxyl groups of γ -Al₂O₃ and the oxygen functionalities of reduced graphene oxide [17].

Fig. 2 b shows the FTIR spectra of pure MgO and MgO samples modified with different amounts of reduced graphene oxide. The spectrum of MgO is characterized by band in the region $500\text{-}400\text{ cm}^{-1}$ attributed to lattice vibrations of Mg-O bonds. In the high-frequency region $3740\text{-}3700\text{ cm}^{-1}$ a narrow band assigned to stretching vibrations of isolated Mg-OH groups is observed, while a broader feature near 3450 cm^{-1} corresponds to hydrogen-bonded O-H groups and adsorbed water on the MgO surface [23]. After deposition of reduced graphene oxide, additional absorption features appear that are absent in pure MgO. A band in the region $1720\text{-}1700\text{ cm}^{-1}$ is assigned to C=O stretching vibrations of carboxyl groups originating from residual oxygen-containing fragments of graphene oxide. In the $1605\text{-}1585\text{ cm}^{-1}$ region a band characteristic of C=C stretching vibrations of the aromatic framework of graphene layers is detected, partially overlapping with the H-O-H bending mode of adsorbed water near 1630 cm^{-1} [24]. The presence of paired bands at about 1550 and 1410 cm^{-1} indicates asymmetric and symmetric stretching vibrations of carboxylate groups coordinated to magnesium, confirming the formation of interfacial Mg-carboxylate species [25]. In the mid-frequency region $1260\text{-}1220\text{ cm}^{-1}$ and $1110\text{-}1040\text{ cm}^{-1}$ bands assigned to C-O-C vibrations of epoxy and ether groups and C-O vibrations of phenolic or alkoxy groups are observed, evidencing the retention of part of the oxygen-containing functionalities and the formation of Mg-O-C type linkages at the interface [26].

Since the modification of MgO was carried out using an aqueous dispersion of reduced graphene oxide, the spectra also reveal a broad O-H stretching band in the $3500\text{-}3700\text{ cm}^{-1}$ region together with a band near 1630 cm^{-1} , characteristic of magnesium hydroxide. These features indicate partial hydration of surface Mg-O groups with the formation of $\text{Mg}(\text{OH})_2$ and the development of a hydroxide-graphene interfacial layer that promotes effective anchoring of graphene sheets on the MgO surface and stabilizes the sample structure.

Fig. 2 c, d shows the Raman spectra of the Al_2O_3 - and MgO-based samples modified with different amounts of reduced graphene oxide (rGO). For all rGO-containing samples, two characteristic bands of graphene materials – the D band ($\sim 1350\text{ cm}^{-1}$) and the G band ($\sim 1580\text{ cm}^{-1}$) – are clearly observed in the $1200\text{-}1600\text{ cm}^{-1}$ region. The ratio of their intensities ($I_{\text{D}}/I_{\text{G}}$), commonly used as a measure of defectiveness in carbon materials, exceeds 1 for all compositions and remains essentially unchanged with increasing rGO loading [18-19]. This indicates that the intrinsic defect level of the deposited graphene phase stays constant regardless of the amount applied to the oxide surface. An increase in the absolute intensity of both D and G bands with higher rGO content reflects the growing concentration of graphene fragments on the supports, while a slight upshift of the G band for Al_2O_3 -based samples may be associated with strain effects within the deposited rGO film [20]. In contrast, the Raman spectra of the pristine oxide supports do not exhibit graphene-related features: the initial $\gamma\text{-Al}_2\text{O}_3$ shows only low-intensity lattice vibrations in the $300\text{-}700\text{ cm}^{-1}$ region, whereas pure MgO displays weak Mg-O lattice modes below 800 cm^{-1} [21-22]. The appearance of D and G bands exclusively after rGO deposition confirms the successful formation of a graphene-based phase on both oxide supports.

Fig. 3 a shows the temperature dependence of acetylene conversion over rGO/ Al_2O_3 catalysts with different graphene oxide loadings. It should be noted that for both alumina and magnesia deposited samples in all catalytic experiments, acetylene hydrogenation proceeded to ethylene, maintaining 100 % selectivity throughout the entire temperature range. No methane or ethane was detected among the reaction products. The rGO 1 mg/ Al_2O_3 sample exhibits the lowest reaction onset at $150\text{ }^\circ\text{C}$ with a conversion of 6 %, reaching 10 % at $250\text{ }^\circ\text{C}$, and decreasing at higher temperatures to 6 % at $400\text{ }^\circ\text{C}$. The rGO 0.1 mg/ Al_2O_3 catalyst becomes active at $200\text{ }^\circ\text{C}$ with a conversion of 0.85 % and shows a

continuous increase in activity up to 13 % at 400 °C. The rGO 0.025 mg/Al₂O₃ sample begins to convert acetylene at about 150 °C with a conversion of 0.4 % and gradually reaches 12 % at 400 °C.

All catalysts exhibit activity within 150-400 °C, with the highest conversion observed for the rGO 0.1 mg/ Al₂O₃ sample at 400 °C.

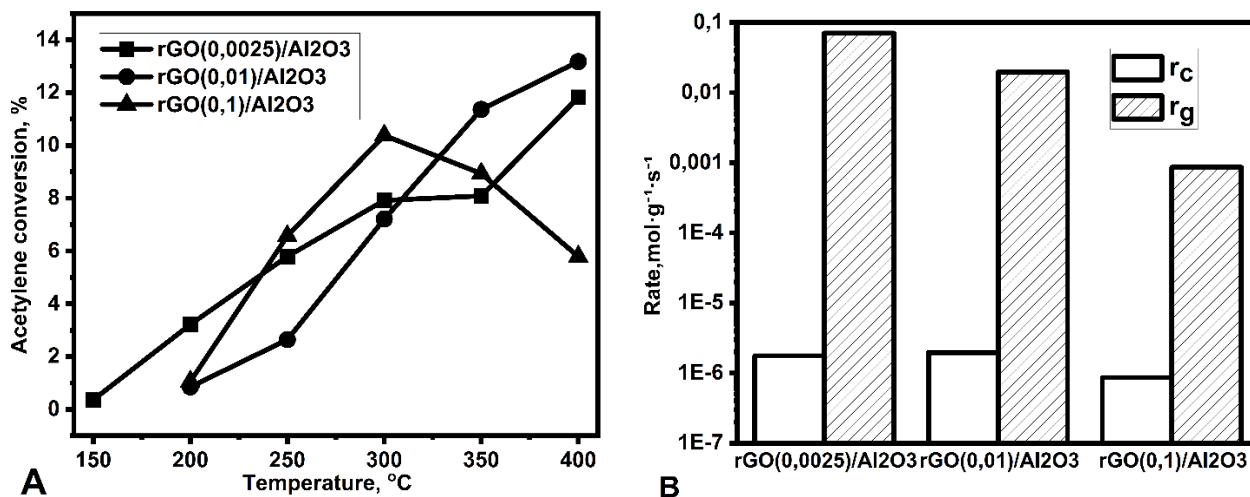


Fig. 3. (a) Temperature dependence of acetylene conversion in the process of acetylene hydrogenation within the temperature range of 50-400 °C, total flow rate 50 mL min⁻¹; ■ conversion of acetylene on rGO(0.025)/Al₂O₃; ● conversion of acetylene on rGO(0.1)/Al₂O₃; ▲ conversion of acetylene on rGO(1)/Al₂O₃. (b) Reaction rate diagrams of acetylene hydrogenation over rGO(0.025)/Al₂O₃, rGO(0.1)/Al₂O₃, and rGO(1)/Al₂O₃, recalculated per catalyst mass and per rGO mass at 400 °C.

r_c - rate of acetylene hydrogenation normalized to the mass of the catalyst sample; r_g - rate of acetylene hydrogenation normalized to the mass of rGO in the catalyst sample

The catalyst with the highest rGO content 0.1 mass. % (1 mg/g) shows the lowest initial temperature for the reaction observed, confirming its superior ability to activate acetylene at low temperatures. However, the intermediate loading (0.1 mg) provides the best balance between activity and thermal stability, achieving the highest conversion at 400 °C. These results indicate that an optimal amount of reduced graphene oxide ensures both efficient low-temperature activation and sustained catalytic performance under thermal conditions.

Fig. 3 b presents the reaction rate diagrams for acetylene hydrogenation at 400 °C using catalysts of the rGO/Al₂O₃ system with different contents of reduced graphene oxide. The reaction rate, calculated per catalyst mass, is 1.8 · 10⁻⁶ mol · g(cat)⁻¹ · s⁻¹ for rGO(0.025)/Al₂O₃, 2.0 · 10⁻⁶ mol · g(cat)⁻¹ · s⁻¹ for rGO(0.1)/Al₂O₃, and 8.6 · 10⁻⁷ mol · g(cat)⁻¹ · s⁻¹ for rGO(1)/Al₂O₃. Thereover, with increasing rGO loading from 0.0025 mass. % to 0.1 mass. %, the activity first increases – reaching a maximum for the 0.01 mass. % rGO sample – and then decreases. When normalized to the mass of reduced graphene oxide, the difference becomes more pronounced: 7.04 · 10⁻² mol · g(rGO)⁻¹ · s⁻¹ for rGO(0.025)/Al₂O₃, 1.96 · 10⁻² mol · g(rGO)⁻¹ · s⁻¹ for rGO(0.1)/Al₂O₃, and 8.62 · 10⁻⁴ mol · g(rGO)⁻¹ · s⁻¹ for rGO(1)/Al₂O₃. This indicates that with increasing rGO content, the specific activity of the catalysts decreases by nearly two orders of magnitude due to densification or partial coverage of the active surface of the support. Therefore, the rGO(0.1)/Al₂O₃ system can be considered optimal, providing the highest reaction rate (1.96 · 10⁻⁶ mol · g(cat)⁻¹ · s⁻¹) and acetylene conversion of 13 % at 400 °C, demonstrating the effective role of the graphene layer in reactant activation.

Fig. 4 a shows the temperature dependence of acetylene conversion over rGO/MgO catalysts with different graphene oxide loadings. The rGO(0.1)/MgO catalyst becomes active at 250 °C with a conversion of 1.4 % and gradually increases to 3.8 % at 400 °C.

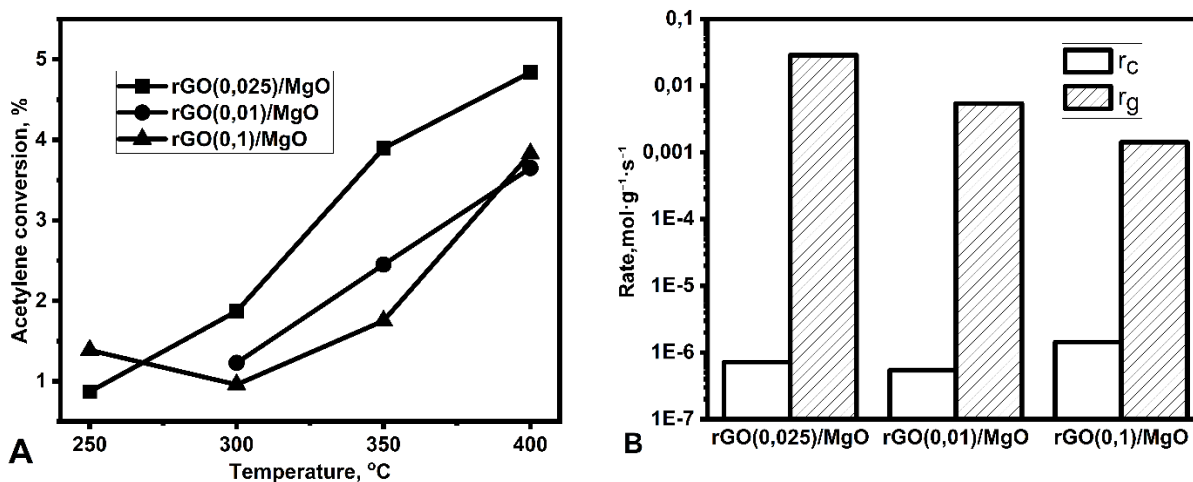


Fig. 4. (a) Temperature dependence of acetylene conversion in the hydrogenation process within the temperature range of 50-400 °C, total gas flow rate 50 mL min⁻¹; ■ Acetylene conversion on rGO(0.0025)/MgO; ● Acetylene conversion on rGO(0.01)/MgO; ▲ Acetylene conversion on rGO(0.1)/MgO. (b) Reaction rate diagrams for acetylene hydrogenation over rGO(0.0025)/MgO, rGO(0.01)/MgO, and rGO(0.1)/MgO, normalized to the catalyst mass and to the mass of rGO.

r_s - rate of acetylene hydrogenation normalized to the catalyst mass;

r_g - rate of acetylene hydrogenation normalized to the mass of rGO in the catalyst sample

The rGO(0.01)/MgO sample starts to convert acetylene at 300 °C with a conversion of 1.2 % and reaches 3.7 % at 400 °C. The rGO(0.0025)/MgO catalyst shows activity from 250 °C with a conversion of 0.9 % and steadily increases to 4.8 % at 400 °C. All rGO/MgO catalysts remain active within 250-400 °C, with the highest conversion observed for the rGO(0.025)/MgO sample at 400 °C. The highest conversion 4.8 % at 400 °C, is achieved for rGO(0.0025)/MgO, indicating that smaller graphene loadings favor better dispersion and stronger interfacial contact with the MgO support. Compared to the rGO/Al₂O₃ system, the MgO-based catalysts demonstrate lower activity but maintain stable performance over the examined temperature interval.

Fig. 4 b shows the reaction rate diagrams for acetylene hydrogenation at 400 °C over rGO/ MgO catalysts with different loadings of reduced graphene oxide. The reaction rate, calculated per catalyst mass, is $7.20 \cdot 10^{-7}$ mol·g(cat)⁻¹·s⁻¹ for rGO(0.0025)/MgO, $5.43 \cdot 10^{-7}$ mol·g(cat)⁻¹·s⁻¹ for rGO(0.01)/MgO, and $1.42 \cdot 10^{-6}$ mol·g(cat)⁻¹·s⁻¹ for rGO(0.1)/MgO. At low rGO contents (0.0025-0.1 mg/g), the catalytic activity remains relatively low, whereas increasing the rGO loading to 1 wt. % leads to nearly a twofold increase in the reaction rate, which can be attributed to the formation of a more continuous graphene coating and improved interfacial contact between MgO and the rGO layer. When normalized to the mass of reduced graphene oxide, the rate values are $2.88 \cdot 10^{-2}$ mol·g(rGO)⁻¹·s⁻¹ for rGO(0.0025)/MgO, $5.43 \cdot 10^{-3}$ mol·g(rGO)⁻¹·s⁻¹ for rGO(0.01)/MgO, and $1.42 \cdot 10^{-3}$ mol·g(rGO)⁻¹·s⁻¹ for rGO(0.1)/MgO. The observed decrease in specific activity with increasing rGO content may result from partial shielding of active centers by graphene layers or from the formation of Mg(OH)₂ during the deposition of rGO from an aqueous suspension.

Therefore, for the rGO/MgO, the highest acetylene hydrogenation rate based on catalyst mass is observed at 400 °C for rGO(0.1)/MgO - $1.42 \cdot 10^{-6}$ mol·g(cat)⁻¹·s⁻¹, although its acetylene conversion

reaches only 4 %. This suggests partial coverage of the active MgO surface or diffusion limitations of reactants within the graphene layer. Meanwhile, the specific activity normalized to the rGO mass for all rGO/MgO samples remains lower than that of analogous γ -Al₂O₃-based systems.

The experiments show that both rGO/Al₂O₃ and rGO/MgO catalysts are active in acetylene hydrogenation, although their temperature-dependent behavior and efficiency differ noticeably. The rGO/Al₂O₃ samples demonstrate higher conversions across the studied temperature range and begin to exhibit measurable activity at lower temperatures. This suggests that γ -Al₂O₃ provides surface conditions more favorable for the surface reaction between adsorbed acetylene and hydrogen [27]. It can be proposed that the presence of surface hydroxyl groups on alumina facilitates stronger interaction between the deposited rGO layers and the oxide surface, providing new or enhancing existing active sites [28].

In contrast, the rGO/MgO catalysts show lower acetylene conversion and require higher temperatures to reach comparable activity trends. The predominantly basic character of MgO results in weaker interaction with the graphene phase, which can be conditioned by interaction between carboxylic groups in OG and MgO due to the first step of deposition [29]. In addition, partial hydration of the MgO surface during deposition from an aqueous rGO suspension leads to the formation of Mg(OH)₂, and interaction of MgO with atmospheric CO₂ can significantly reduce the surface hydrogen migration due to poisoning of the surface by blocking -OH groups [30]. This modification of the surface composition limits hydrogen surface mobility and contributes to lower overall activity. Nevertheless, all MgO-based catalysts retain stable operation throughout the reaction temperature range.

Across both systems, the amount of deposited reduced graphene oxide is a key factor in determining catalytic behaviour. Lower rGO loadings ensure better dispersion and a more open surface, whereas higher loadings may lead to partial coverage of the oxide grains and restricted access to active regions. This effect is more pronounced for MgO, where thicker graphene layers can hinder contact between reactants and the basic surface sites [31-32]. In the Al₂O₃-supported samples, moderate rGO loadings improve catalytic performance while preserving the structural accessibility of the support.

Conclusions

Therefore, the obtained results show that the optimal content of reduced graphene oxide lies in the range of 0.025-0.1 mg, which provides a balance between low-temperature activity and thermal stability of the catalytic system. Among the investigated samples, the rGO 0.1 mg/Al₂O₃ catalyst provides the highest acetylene conversion of 13 % at 400 °C, with 100 % selectivity to ethylene and stable performance throughout the reaction. Overall, the observed trends indicate that the catalytic behavior of graphene-oxide catalysts is mainly determined by the acid-base properties of the support and the structural characteristics of the rGO layer, which together influence both the temperature required for activation and the thermal stability of the system. The results obtained may serve as a basis for the rational design of metal-free or low-metal hydrogenation catalysts for selective transformations of unsaturated hydrocarbons.

References

1. Studt F., Calle-Vallejo F., Luo J., Hansen H.A., Nørskov J.K., Bligaard T. On the role of surface structure for catalyst selectivity by first-principles theory. *ChemCatChem*, 2012, **4**(11), 1809–1815.
2. Borodziński A., Bond G.C. Selective hydrogenation of ethyne in ethene-rich streams on palladium catalysts. Part 1: Oxide supports. *Catal. Rev.*, 2006, **48**(1), 91–144.

3. Liu Y., Wang Z., Zhang X. Review on graphene-based metal-free catalysts: Synthesis and applications. *Chem. Eng. J.*, 2015, **270**, 1–25.
4. Chen X., Park J., Ruoff R.S. Chemical functionalization of graphene and its applications. *Chem. Rev.*, 2016, **116**(14), 704–711.
5. Dreyer D.R., Park S., Bielawski C.W., Ruoff R.S. The chemistry of graphene oxide. *Chem. Soc. Rev.*, 2010, **39**(1), 228–240.
6. Loh K.P., Bao Q., Eda G., Chhowalla M. Graphene oxide as a chemically tunable platform for optical applications. *Nat. Chem.*, 2010, **2**(12), 1015–1024.
7. Stankovich S., Dikin D.A., Piner R.D., et al. Synthesis of graphene-based nanosheets via chemical reduction of exfoliated graphite oxide. *Carbon*, 2007, **45**(7), 1558–1565.
8. Abakumov A., Bychko I.B., Selyshchev O.V., Zahn D.R.T., Qi X., Tang J., Stryzhak P.Ye. Highly selective hydrogenation of acetylene over reduced graphene oxide carbocatalyst. *Materialia*, 2021, **18**, 101163.
9. Zhu C., Sheng J., Lu R. Metal-free hydrogenation of alkynes using nitrogen-doped graphene as a catalyst. *ACS Catal.*, 2018, **8**(10), 10081–10088.
10. Primo A., Neatu F., Florea M., Parvulescu V., Garcia H. Graphenes in the absence of metals as carbocatalysts for selective acetylene hydrogenation and alkene hydrogenation. *Nat. Commun.*, 2014, **5**, 5291.
11. Nosach V.V., Bychko I.B., Stryzhak P.Ye. Catalytic properties of reduced graphene oxide deposited on aluminum oxide in ethane dehydrogenation. *Theor. Exp. Chem.*, 2025, **61**(2), 121–126. [in Ukrainian].
12. Kheirandish E., Taherzadeh M. Quasi-2D crystalline γ -alumina grown by graphene-templated method. *Adv. Mater. Interfaces*, 2020, **7**(3), 2000561.
13. Gómez-Navarro C., Burghard M., Kern K. Atomic structure of reduced graphene oxide. *Nano Lett.*, 2010, **10**(4), 1144–1148.
14. Long Y., Zhang Z., Zhao X., Wang D. Field emission of MgO-coated graphene sheets prepared by atomic layer deposition. *J. Vac. Sci. Technol. B*, 2015, **33**(1), 012204.
15. Busca G. Acid-base properties of metal oxide surfaces and their characterization by IR spectroscopic methods. *Adv. Catal.*, 2014, **57**, 319–404.
16. Navalon S., Dhakshinamoorthy A., Alvaro M., García H. Carbocatalysis by graphene-based materials. *Chem. Rev.*, 2014, **114**(12), 6179–6212.
17. Acik M., Lee G., Mattevi C., Chhowalla M., Cho K., Chabal Y.J. Unusual infrared-absorption mechanism in thermally reduced graphene oxide. *Nat. Mater.*, 2010, **9**(10), 840–845.
18. Ferrari A.C. Raman spectroscopy of graphene and graphite: Disorder, electron-phonon coupling, doping and nonadiabatic effects. *Solid State Commun.*, 2007, **143**(1–2), 47–57.
19. Eckmann A., Felten A., Mishchenko A., Britnell L., Krupke R., Novoselov K.S., Casiraghi C. Probing the nature of defects in graphene by Raman spectroscopy. *Nano Lett.*, 2012, **12**(8), 3925–3930.
20. Mohiuddin T.M.G., Lombardo A., Nair R.R., Bonetti A., Savini G., Jalil R., Ferrari A.C. Uniaxial strain in graphene by Raman spectroscopy. *Phys. Rev. B*, 2009, **79**(20), 205433.
21. Busca G. The surface of transitional aluminas: A critical review. *Catal. Today*, 2014, **226**, 2–13.
22. Gotić M., Ivanda M., Sekulić A., Musić S., Matthews A., Popović S. Raman spectroscopic study of MgO and Mg(OH)₂ under high pressure. *J. Mol. Struct.*, 2000, **555**(1–3), 353–360.
23. Frost R.L., Klopogge J.T. Vibrational spectroscopy of hydroxyl groups in MgO-H₂O system. *Spectrochim. Acta A*, 1999, **55**(12), 2195–2205.
24. Liu P., Yan Y. Preparation and characterization of reduced graphene oxide and its composite with TiO₂ by FTIR and Raman spectroscopy. *Appl. Surf. Sci.*, 2010, **256**(9), 2810–2814.
25. Reddy B.M., Khan A. Promoted MgO catalysts for organic transformations: FTIR characterization of carbonate and carboxylate species on MgO. *J. Mol. Catal. A*, 2005, **230**(1–2), 33–39.
26. Hu Y., Shen J., Li N., Ma H., Shi M., Ye M. Microwave-assisted reduction and functionalization of graphene oxide on MgO surfaces. *J. Phys. Chem. C*, 2010, **114**(20), 9308–9313.

27. Gao J., Chen S., Wang H. Effect of support acidity on catalytic performance of Pt-based catalysts for selective hydrogenation of acetylene. *Catal. Today*, 2017, **295**, 110–118.
28. Santos A.L.R., et al. Quantification of hydroxyl groups on alumina supports and their role in catalytic activity. *Braz. J. Anal. Chem.*, 2018, **5**(20), 48–59.
29. Kwon O., Park J., Kim J., Song I. Acid-base properties of metal oxides and their influence on catalytic hydrogenation reactions. *J. Mol. Catal. A*, 2015, **398**, 156–164.
30. Busca G. Bases and basic materials in heterogeneous catalysis: MgO, CaO, hydrotalcites and related materials. *Catal. Today*, 2009, **143**, 2–8.
31. Torshizi H.O., Nakhaei Pour A., Mohammadi A., Zamani Y., Shahri S.M.K., Kamali Shahri S.M. Fischer-Tropsch synthesis by reduced graphene oxide nanosheets supported cobalt catalysts. *Front. Chem. Sci. Eng.*, 2021, **15**, 299–309.
32. Grigoriev S.A., et al. Reduced graphene oxide (RGO) and its modifications as catalyst supports: Effects of loading and layer thickness. *Materials*, 2018, **11**(8), 1405.

Надійшла до редакції 20.11.2025

Каталітичні властивості відновленого оксиду графену, нанесеного на оксиди алюмінію та магнію, у реакції гідрування ацетилену

Вікторія В. Носач^{1,2}, Ігор Б. Бичко¹, Петро Є. Стрижак¹

¹ Інститут фізичної хімії ім. Л.В. Писаржевського Національної академії наук України
просп. Науки, 31, Київ, 03028, Україна

² Національний університет «Києво-Могилянська академія»
вул. Григорія Сковороди, 2, Київ, 04655, Україна, e-mail: victorynosach@gmail.com

Каталітичні властивості відновленого оксиду графену (ВОГ), нанесеного на оксиди алюмінію та магнію, були досліджені в реакції гідрування ацетилену. Каталізатори з різним вмістом ВОГ отримували методом просочення γ -Al₂O₃ та MgO водними суспензіями оксиду графену з подальшим відновленням у водні за 400 °С. Матеріали характеризували за допомогою Фур'є-ІЧ спектроскопії (ІЧ), Раманівської спектроскопії та СЕМ. ІЧ-спектри підтвердили успішне нанесення rGO на обидві підкладки, а для зразків на основі MgO також виявили часткову гідратацію поверхневих Mg–O груп з утворенням Mg(OH)₂ та гідроксидно-графенового міжфазного шару, який покращує закріплення та стабілізує структуру. За допомогою Раманівської спектроскопії було підтверджено формування графенвмісної фази на обох оксидах і показано, що рівень дефектності осажденного графену залишається постійним при зміні вмісту ВОГ. Аналіз зображень СЕМ виявив, що на ВОГ/MgO утворює тонкі плівкоподібні структури та нерегулярні складки, які формують частково покриті ділянки, тоді як на γ -Al₂O₃ він утворює безперервні плівки в одних зонах і ізольовані складки в інших. Модифікація γ -Al₂O₃ та MgO відновленим оксидом графену підвищила каталітичну активність зразків гідруванні ацетилену, причому найвищі швидкості спостерігалися для зразків із низьким вмістом ВОГ. Обидва каталізатори – ВОГ/Al₂O₃ та ВОГ/MgO – продемонстрували повну (100 %) селективність за етиленом в діапазоні 250–400 °С. Підвищення активності пояснюється наявністю поверхневих структур, утворених ВОГ, які забезпечують ефективний контакт між вуглецевою та оксидною фазами й сприяють активації ацетилену та водню. Загалом каталітична активність оксидів, модифікованих ВОГ, визначається кислотно-основними властивостями носія та структурними особливостями нанесеного графенового шару, які задають температуру активації та термічну стабільність системи.

Ключові слова: відновлений оксид графену, оксид алюмінію, оксид магнію, гідрування ацетилену, каталіз